

which contains other, possibly more intrinsic sources of crystallinity deficiency."

Because of the large specific surface area of single crystals,²³ $\sim 10^6$ cm² g⁻¹ one might imagine that the hydrogen solubility in the single crystals could be accounted for by assuming complete surface coverage to the depth of one layer. However, taking the molecular diameter of the hydrogen molecule²⁴ as 2.19 Å it is easy to calculate that a surface of 10^6 cm² g⁻¹, would accommodate 9×10^{-1} g of H₂/100 g of the single crystals. This is almost three orders of magnitude larger than the actually observed solubility (Table V) and demonstrates that the interlamellae surfaces are certainly sufficiently great enough in area to sorb the dissolved hydrogen. Of course, there is nothing approaching a surface coverage at 1-atm pressure otherwise a Langmuir sorption isotherm would be deduced from the data. Furthermore, one would hardly expect the simple Flory-Huggins mixing theory to be applicable to the mixing of hydrogen or helium molecules with the interlamellae folded-chain structure of the polyethylene. The entropy of mixing from Figure 7 is surprisingly high for the single crystal sample, and if this result is correct, it would indicate that more configurations are available to the system of gas molecules and polyethylene segments than in the case of the other PE samples; in other words per gram of amorphous polymer there are more sorption sites for the hydrogen and helium molecules in the case of the single crystals.

Acknowledgments. This research was supported by the U. S. Atomic Energy Commission and by income from the chair in chemistry at Baylor University endowed by a gift from The Robert A. Welch Foundation. Dr. J. A. Reid of the Phillips Petroleum Co. kindly supplied the Marlex-6002 polyethylene and Professor B. Wunderlich of Rensse-

laer Polytechnic Institute the samples of high-pressure-crystallized polyethylene.

References and Notes

- (1) A. S. Michaels and R. B. Parker, Jr., *J. Phys. Chem.*, **62**, 1604 (1958).
- (2) A. S. Michaels and H. J. Bixler, *J. Polym. Sci.*, **50**, 393 (1961).
- (3) N. G. McCrum, *Polymer*, **5**, 319 (1964).
- (4) P. N. Lowell and N. G. McCrum, *Polym. Lett.*, **5**, 1145 (1967).
- (5) T. M. Deas, Jr., H. H. Hofer, and M. Dole, *Macromolecules*, **5**, 223 (1972).
- (6) K. Toi, T. Kaminaga, and T. Tokuda, *Kogyo Kagaku Zasshi*, **73**, 1467 (1970).
- (7) A. S. Michaels, W. R. Vieth, and J. A. Barrie, *J. Appl. Phys.*, **34**, 1 (1963).
- (8) W. R. Vieth and K. J. Sladek, *J. Colloid Sci.*, **20**, 1014 (1965).
- (9) W. R. Vieth, C. S. Frangoulis, and J. A. Rionda, Jr., *J. Colloid Interface Sci.*, **22**, 454 (1966).
- (10) S. Kubo and M. Dole, *Macromolecules*, **6**, 774 (1973).
- (11) W. Y. Wen, D. R. Johnson, and M. Dole, to appear in *Macromolecules*.
- (12) P. Meares, "Polymers: Structure and Bulk Properties," D. Van Nostrand, London, 1965, p 320.
- (13) R. Ash, P. M. Barrer, and D. G. Palmer, *Polymer*, **11**, 421 (1970).
- (14) F. Namada, B. Wunderlich, T. Sumida, S. Hayashi, and A. Nakajima, *J. Phys. Chem.*, **72**, 178 (1968).
- (15) M. Dole, *J. Chem. Phys.*, **16**, 25 (1948).
- (16) S. Brunauer, P. H. Emmett, and E. Teller, *J. Amer. Chem. Soc.*, **69**, 651 (1947).
- (17) M. Dole and A. D. McLaren, *J. Amer. Chem. Soc.*, **69**, 651 (1947).
- (18) See, for example, E. A. Guggenheim, "Mixtures," Oxford Univ. Press, Oxford, 1952, p 252.
- (19) This treatment is similar in some respect to that of R. J. Roe, H. E. Bair, and C. Gieniewski, to be published. See also *Polym. Prepr., Amer. Chem. Soc., Div. Polym. Chem.*, **14**, 530 (1973).
- (20) See ref 18, p 253.
- (21) V. S. Kogan, B. G. Lazarev, and R. F. Bulatova, *Zh. Eksp. Teor. Fiz.*, **37**, 678 (1959).
- (22) Y. Udagawa and A. Keller, *J. Polym. Sci., Part A-2*, **9**, 437 (1971).
- (23) B. Wunderlich, "Macromolecular Physics," Academic Press, New York, N. Y., 1973, Vol. 1, p 387.
- (24) W. J. Moore, "Physical Chemistry," Prentice Hall, Inc., Englewood Cliffs, N. J., 1962, 3rd ed, p 229.

Radiation Chemistry of Polyethylene. XIII.¹ Alkyl Radical Decay Kinetics in Single Crystalline and Extended-Chain Samples of Linear Polyethylene

Walter Y. Wen, David R. Johnson, and Malcolm Dole*

Department of Chemistry, Baylor University, Waco, Texas 76703. Received November 30, 1973

ABSTRACT: In this paper the previous kinetic study of alkyl free-radical decay in bulk polyethylene (PE) has been broadened to include a study of single crystalline and extended-chain samples of PE. At room temperature and above the decay kinetics can be quantitatively expressed in terms of two simultaneous first-order decay reactions. The catalytic effect of hydrogen gas on the radical decay rate is very much greater in single crystalline PE than in bulk, but the enhanced catalytic activity is in line with the approximately 10-fold greater solubility (per unit of amorphous content) of hydrogen in the single crystal samples. In the extended-chain samples the hydrogen catalytic effect was less than expected. Activation energies decrease with increasing crystallinity of the samples and the activation energies of the fast decay approach those of the slow decay with decreasing crystallinity.

Using samples of bulk polyethylene (PE) of different amorphous volume fractions, α_v , Johnson, Wen, and Dole¹ showed that the decay of alkyl radicals at room and higher temperatures could be expressed in terms of two first-order decay reactions with constants k_f for the fast decay and k_s for the slow decay. Both of these constants increased as α_v increased. Furthermore, molecular hydrogen had a pronounced catalytic effect on both the slow and fast decays. Inasmuch as hydrogen is soluble only in the amorphous regions of the PE^{2,3} it appears that most, if not all, of the alkyl decay at room or higher temperatures must occur in the amorphous regions. This last statement

is also supported by the fact that allyl radicals produced at room temperature by the reaction of a free-radical center and a double bond are mostly (70% or higher) of the chain end type when the decay is studied after γ -ray doses of 27 Mrads or less where the vinyl groups still have a significant concentration.⁴ It is known that 90% of the vinyl end groups are located in the amorphous zones, at least in single crystalline (SC) PE.⁵

With respect to other papers dealing with the decay kinetics of alkyl radicals in PE, several reviews⁶⁻⁸ have been published so that older work will not be referred to here unless pertinent.

Table I
Densities and Amorphous Volume Fractions at
25° of Polyethylene Samples Studied

Sample	Sample Designation ³	Density	α_v
Single crystals	S-1	0.9782	0.143
Extended chain	P-L	0.9900	0.062
Extended chain	P-M	0.9938	0.036

Recently we have found³ that per unit of amorphous content (as calculated from density measurements) molecular hydrogen is considerably more soluble in SC and extended-chain (EC) PE than expected on the basis of its solubility in bulk PE. Hence it became of considerable interest to see if the enhanced hydrogen solubility also produced an enhanced catalytic effect on the alkyl radical decay in these types of PE. We also wished to study the effect of the different types of crystallinity on the alkyl radical decay *in vacuo*. As demonstrated below relationships between the activation energies and entropies of the alkyl radical decay and amorphous content can be shown to exist.

I. Experimental Section

A. Materials. The SC samples of PE in the form of mats were prepared from Marlex-6002 PE by crystallization at 90° from a 0.2 wt % solution of PE in xylene. Electron micrographs of the samples showed typical single crystal layering. EC samples³ were kindly donated by Professor B. Wunderlich of Rensselaer Polytechnic Institute. Densities were determined³ to ± 0.001 density unit at 25° in a toluene-monochlorobenzene density gradient column, and the amorphous volume fraction, α_v , calculated by means of the previously used equation.¹ Data for the different samples are collected in Table I.

B. Irradiation and Computer Techniques. All irradiations were carried out in a Co-60 γ -ray source at 77°K *in vacuo* at a dose rate of about 0.25 Mrad hr⁻¹. The esr signals produced in the quartz irradiation tubes were annealed out before making the alkyl radical concentration measurements as previously described.¹ Other irradiation details, the handling of the irradiated samples and the computer techniques for data acquisition and smoothing were also as previously published.¹ As an esr standard we chose for this work a mixture of DPPH (diphenylpicrylhydrazyl) powder in KCl powder. The latter was Beckman electrode grade and was dried in a vacuum oven. The ratio of the spin moments of this standard sample at 116 and 293°K was 2.13 whereas the ratio of temperatures, 293 and 116°K is 2.52. According to Poole⁹ the area under an esr spectrum should be inversely proportional to the absolute temperature at which the spectrum is measured.

II. Kinetic Treatment of Data and Results

A. Alkyl Radical G Values. The concentrations of the alkyl radicals produced by irradiation at 77°K as a function of dose for both the S-1 and P-M samples of PE are illustrated in Figure 1. The concentrations are linear with dose up to doses of 30 Mrads and from the slopes of the lines $G(R\cdot)$ was calculated to be 4.46 ± 0.34 for the SC sample, S-1, and 3.33 ± 0.07 for the EC sample, P-M. The latter G value is practically identical with that, 3.32 ± 0.26 , found for $G(R\cdot)$ in bulk PE,¹ but the SC G value for the alkyl radicals is definitely higher. This is possibly due either to the difficulty of radical recombination in the crystalline zones of the single crystals during the irradiation at 77°K, or to a greater formation of chain end free radicals which are produced⁶ in bulk PE by the irradiation at 77°K to the extent of about 10% of the alkyl free radicals. Another possibility suggested by Kusumoto *et al.*¹⁰ is that the radicals are trapped and concentrated at the crystal surfaces of the single crystals.

B. Decay Kinetics. In agreement with the observations¹ on bulk PE, the alkyl radical decay kinetics can be

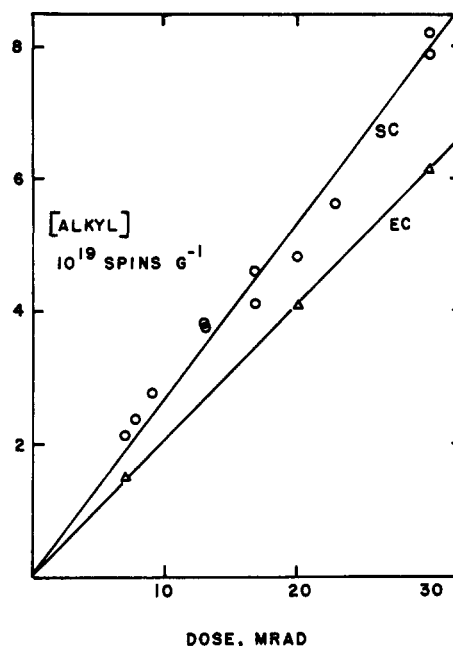


Figure 1. Production of alkyl radicals in polyethylene on γ irradiation at 77°K. Esr measurements at 116°K. Circles, single crystal sample, S-1; triangles, extended-chain sample, P-M, of $\alpha_v = 0.062$.

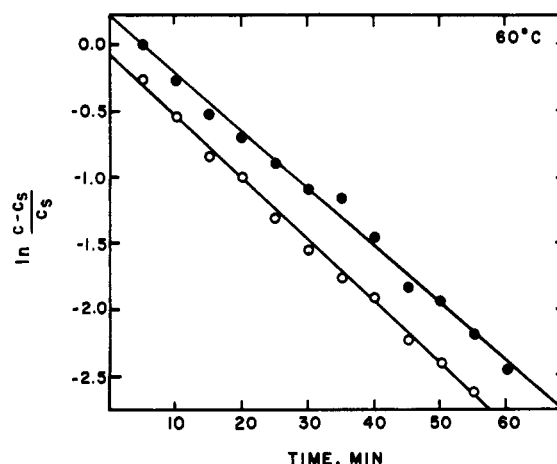


Figure 2. Two simultaneous first-order decay plots of alkyl radicals at 60° *in vacuo*; open circles, 8.6-Mrad dose; solid circles, 22.8-Mrad dose. Single crystals of $\alpha_v = 0.143$, sample S-1.

quantitatively expressed by two simultaneous first-order decay processes, one a fast decay with first-order decay constant, k_f , and the other a slow decay with constant, k_s . Combining the two first-order expressions, we obtained¹ the equation

$$\ln [(c - c_s)/c_s] = \ln (c_f^0/c_s^0) - (k_f - k_s) t \quad (1)$$

where c is the total alkyl radical concentration at time t and c_f^0 and c_s^0 are the initial free-radical concentrations of the fast and slowly decaying radicals, respectively. At long times the decay is essentially that of the slowly decaying radicals when k_s can be determined. Using k_s , c_s at short times can be calculated and $\ln [(c - c_s)/c_s]$ then plotted as a function of t . Figure 2 illustrates such a plot for SC PE for the decay at 60° *in vacuo* and Figure 3 for the EC sample at 40°. By the least-squares method the constants $k_f - k_s$ and c_f^0/c_s^0 can be calculated from the slope and intercept, respectively, and knowing k_s and c_s^0 , k_f and c_f^0 readily follow. In both Figures 2 and 3 the open circle data represent alkyl decay kinetics after a dose of

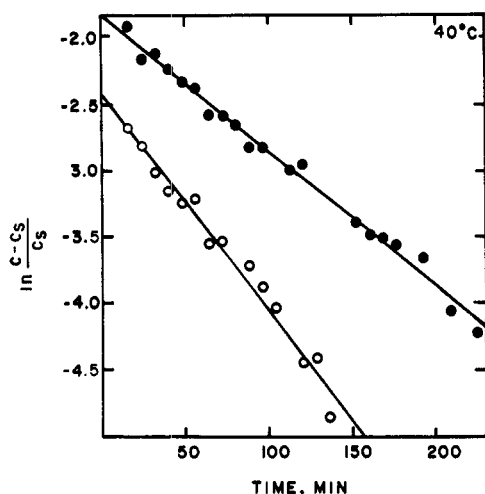


Figure 3. Same as Figure 2 except for decay at 40° in extended-chain crystals of $\alpha_v = 0.036$, sample P-M.

8.6 Mrads and the closed circles after a dose of 22.8 Mrads, both irradiations *in vacuo* at 77°K. The fraction of alkyl radicals surviving the heating to 25° after 10 min was $30.4 \pm 4.8\%$ in the SC samples (average of 14 experiments) and $26.8 \pm 5.8\%$ in the EC samples (average of 3 experiments).

In contrast to the data obtained with the bulk PE, the data at the two different doses did not overlap, but the overlap was closer in the SC than in the EC sample. For an exact overlap to occur it is necessary that the ratio of the initial concentrations of the fast and slowly decaying radicals be equal at the different doses and that $(k_f - k_s)$ be unaffected by dose. The slopes and intercepts are nearly equal for the single crystal data, but the divergences are greater for the extended-chain sample. Data for k_f , k_s , and c_f^0/c_s^0 obtained under a variety of conditions are collected in Table II.

III. Discussion

A. Decay Constants and Amorphous Volume Fractions. Johnson *et al.*¹ previously found that in bulk PE k_s was proportional to α_v ,² but in the present research there were not enough SC or EC samples to test thoroughly this relationship. However, enough data were obtained to show that the k_s/α_v ratio was not constant when a comparison of these ratios for the bulk film ($\alpha_v = 0.272$), SC and EC samples was carried out for data at 60° *in vacuo*. Thus, the ratios were, in units of 10^{-3} sec^{-1} , 1.4, 8.4, 8.4, and 13.9 for the bulk film, SC, EC ($\alpha_v = 0.062$ and 0.036) samples. There is a rough increase of these ratios with increase of crystallinity. Actually, there is a better correlation between the k_s/α_v ratios. These ratios in units of 10^{-4} sec^{-1} and in the same order were 3.9, 12.0, 5.2, and 5.0 for the four different samples. On the basis of this comparison the slow decay in the single crystals is about twice as rapid as in the other samples and probably is the result of the layered structure of the amorphous zones. However, in the case of the fast decay constants, which in the Johnson *et al.*¹ research were very scattered when plotted as a function of α_v ,² the k_f/α_v ratios in units of 10^{-4} sec^{-1} were 17, 64, 86, and 63, respectively. In this comparison the fast decay in the bulk film per unit of amorphous volume is considerably slower than in either the SC or EC PE samples.

When the initial alkyl radical concentrations at the start of the decay process, say at 60°, are compared, the EC samples have the highest radical concentration if all of the radicals are assumed to be in the amorphous zones.

Table II
Kinetic Data for the Decay of Alkyl Radicals
in Single Crystalline and Extended-Chain
Samples of Linear Polyethylene

Dose (Mrads)	H ₂ Pres- sure (Torr)	Temp (°C)	$\times 10^4 \text{ sec}^{-1}$ k_f	k_s	c_f^0/c_s^0	k_s/k_f
Single Crystal Sample (S-1) $\alpha_v = 0.143$						
23.0	0	35	3.14	0.28	0.3	0.089
22.8	0	40	3.98	0.38	0.5	0.095
16.8	0	45	5.55	0.58	0.4	0.105
8.6	0	50	8.27	1.45	0.5	0.175
9.1	0	50		1.75		
16.8	0	55	11.85	2.13	0.4	0.180
13.0	0	60	9.72	1.93	1.4	0.199
22.8	0	60	11.58	1.93	1.4	0.167
30.0	0	60	6.13	1.28	1.5	0.209
7.0	0	65	13.38	3.43	1.0	0.256
20.0	100	25	13.50	2.50	0.1	0.185
30.0	200	25	14.97	2.47	0.6	0.165
30.0	200	25	20.49	3.61	0.3	0.176
20.0	400	25		7.24		
7.0	600	25		11.41		
Extended-Chain Sample (P-M) $\alpha_v = 0.036$						
8.6	0	40	2.78	0.07	0.1	0.025
22.8	0	40	1.77	0.07	0.2	0.040
8.6	0	60	2.25	0.18	0.2	0.080
20.0	0	70	3.63	0.50	0.4	0.138
22.8	600	40	4.83	0.90	1.0	0.186
Extended-Chain Sample (P-L) $\alpha_v = 0.062$						
14.0	0	60	5.35	0.32	0.4	0.060
30.0	200	60	12.69	3.16	0.7	0.249
20.0	400	60	19.34	4.01	0.3	0.207
7.0	600	25	2.97	0.34	0.3	0.114
7.0	600	60		2.66		

But the alkyl radical decay constants are smallest for the EC samples; hence initially all of the radicals cannot be in the amorphous zones. We consider this point again below.

B. Catalytic Effect of Molecular Hydrogen. The catalytic effect of molecular hydrogen in increasing both the k_f and k_s decay constants is illustrated in Figure 4 for the bulk and SC samples and in Figure 5 for the EC samples. Because molecular hydrogen is considerably more soluble³ in single crystalline and EC PE per unit of amorphous content than in bulk PE, comparisons of the catalytic effect of hydrogen between the three types of materials should be made on the basis of the actual concentration of the dissolved hydrogen in the amorphous regions. Such a comparison is made in Table III, where σ_a is the solubility of the hydrogen at 600-Torr pressure/unit of amorphous volume. The k_s/σ_a or k_f/σ_a ratios are the same order of magnitude when comparisons are made between the SC and bulk film samples, but the two ratios are approximately an order of magnitude lower in the case of the EC sample. It should be mentioned that the k_f estimate for the SC sample was obtained approximately by means of a rather uncertain extrapolation of the data at 100 and 200 Torr to 600 Torr of hydrogen. At 600 Torr of hydrogen the fast decay of the alkyl radicals in the SC was too rapid to measure accurately. The slow decay constants were linear with hydrogen pressure as can be seen from Figure 4; hence it was assumed that this would also be true for the k_f values. The approximate although definite correlation between the alkyl radical decay and the hydrogen solubilities indicates that the measured high solubility of hydrogen in the SC represents a true solubility; otherwise the hydrogen would not have such a marked catalytic effect. Thus, if the hydrogen were adsorbed only on the surface of

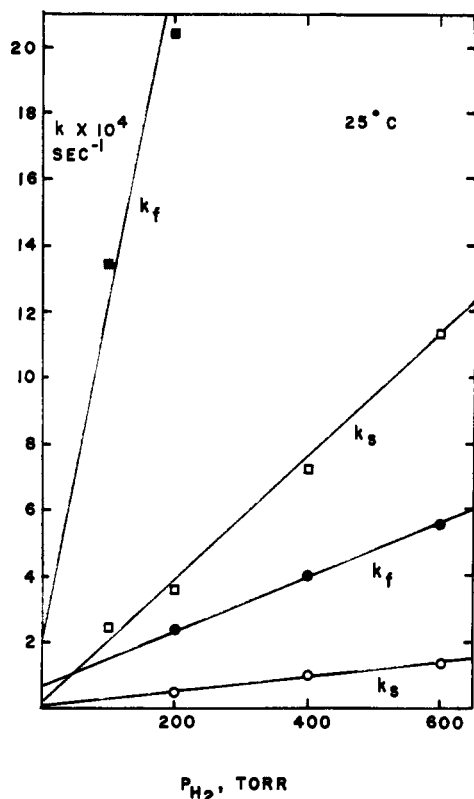


Figure 4. Comparison of catalytic effect at 25° of hydrogen on the fast and slow decay processes in bulk PE, $\alpha_v = 0.272$, circles and in the single crystal sample, S-1, squares.

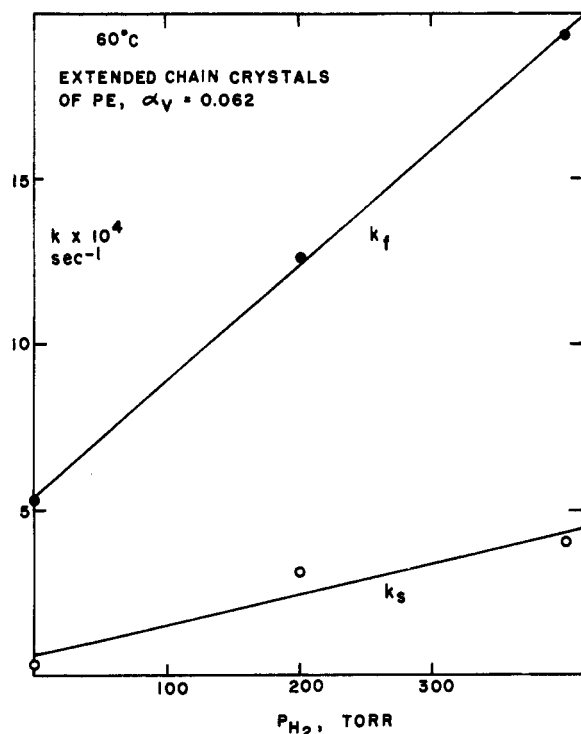


Figure 5. Same as Figure 4 but for the extended-chain sample of $\alpha_v = 0.062$ at 60°, sample P-L.

the SC, one would not expect such a strong, if any, catalytic effect on the alkyl radical decay.

The hydrogen catalysis of the decay of the alkyl radicals in the EC sample is much lower than in the other samples. It may be that at 25° the diffusibility of the hydrogen in the EC sample was low enough to affect its catalytic activity. In the hydrogen solubility studies,³ it was

Table III
Comparison of the Catalytic Effect of Hydrogen on the Slow and Fast Decay Constants (25° and 600-Torr Pressure)

Sample	α_v	σ_a^a	k_s^b	k_f^b	k_s/σ_a^c	k_f/σ_a^c
Bulk film	0.272	2.79	1.41	5.54	0.51	2.0
Single crystal	0.143	31.2	11.4	50-55	0.37	1.6-1.8
Extended chain	0.062	9.3	0.34	2.97	0.04	0.3

^a g of H₂/g of amorphous PE $\times 10^6$. ^b sec⁻¹ $\times 10^4$. ^c g of amorphous PE g_{H₂}⁻¹ sec⁻¹ $\times 10^{-2}$.

found necessary to allow a longer time for hydrogen solubility equilibrium to be attained than in the case of the bulk film or SC samples, but we do not have accurate hydrogen diffusion coefficients in the three types of PE for comparison. The low hydrogen catalytic activity in the EC PE is in line with the conclusion of the previous section that in the EC samples initially the alkyl radicals are segregated in crystalline zones to a greater extent than in the case of the bulk film or SC samples. This may be a more reasonable explanation than that based on the low diffusibility of the hydrogen in the EC sample. If the hydrogen diffusibility were rate determining, then we should expect the catalytic effect of hydrogen per unit of concentration in the amorphous phase to be much greater in the SC samples because Kubo and Dole³ found an extremely rapid rate of diffusion of hydrogen into and out of the SC mats. It should also be realized that at an ambient pressure of 600 Torr of hydrogen initially there is about a two orders of magnitude greater free-radical concentration in the PE at the start of the decay process than concentration of hydrogen molecules (both concentrations calculated assuming all free radicals and dissolved hydrogen to be in the amorphous zones) except for the SC samples where the initial free-radical concentration was only about 17-fold greater than the molecular hydrogen concentration. The "mean free path" of the hydrogen molecules between collisions with free radicals should be very small and of the order of $c_0^{-1/3}$ or about 37 Å initially in the SC sample after a dose of 30 Mrads. Moore¹¹ gives the simple relation, $\bar{x}^2 = 2Dt$, for the calculation of the average square of the diffusing distance in the x direction of gas molecules in a solid if the diffusion coefficient, D , and time, t , are known. Here we calculate the time to travel the distance 37 Å assuming a value² of D equal to ca. 2×10^{-6} cm² sec⁻¹. We find approximately 0.03 μ sec; hence it would appear that diffusion is not rate limiting inasmuch as the free radicals decay over periods of many minutes.

C. Energies and Entropies of Activation. In our previous paper¹ we showed that both $\ln k_s$ and $\ln k_f$ were linear functions of $1/T$ yielding similar activation energies in the case of the bulk PE equal to about 17 kcal mol⁻¹. But in the case of the SC and EC samples, the activation energies for the slow and fast decay process were not equal, see Figure 6. Data for E_a are collected in Table IV where it can be seen that in the case of the SC sample the activation energy for the slow decay process is the same as in the bulk PE; hence we can conclude that the decay mechanisms are essentially identical in these two cases. But the activation energy for the fast process in the SC sample and for both the fast and slow processes in the EC sample are significantly less than E_a for the bulk PE. If a plot is made of E_a as a function of α_v , the activation energies for the fast and slow processes approach each other as α_v increases. If the alkyl free-radical decay rate is deter-

Table IV
Activation Energies and Preexponential Factors for the First-Order Alkyl Radical Decay Processes
in Bulk Single Crystalline and Extended-Chain Samples of Polyethylene

Sample Type	α_v	E_a (kcal mol ⁻¹)		A (sec ⁻¹)	
		Slow	Fast	Slow	Fast
Bulk film ¹	0.373	18.3 ± 1.0	16.4 ± 0.7	2.2 × 10 ⁸	6.8 × 10 ⁷
	0.272	17.0 ± 1.1	16.4 ± 1.1	1.5 × 10 ⁷	3.1 × 10 ⁷
Single crystal	0.143	17.4 ± 1.6	10.2 ± 1.1	5.9 × 10 ⁷	5.6 × 10 ³
Extended chain	0.036	13.7 ± 2.9	4.7 ± 2.0	2.3 × 10 ⁴	0.32

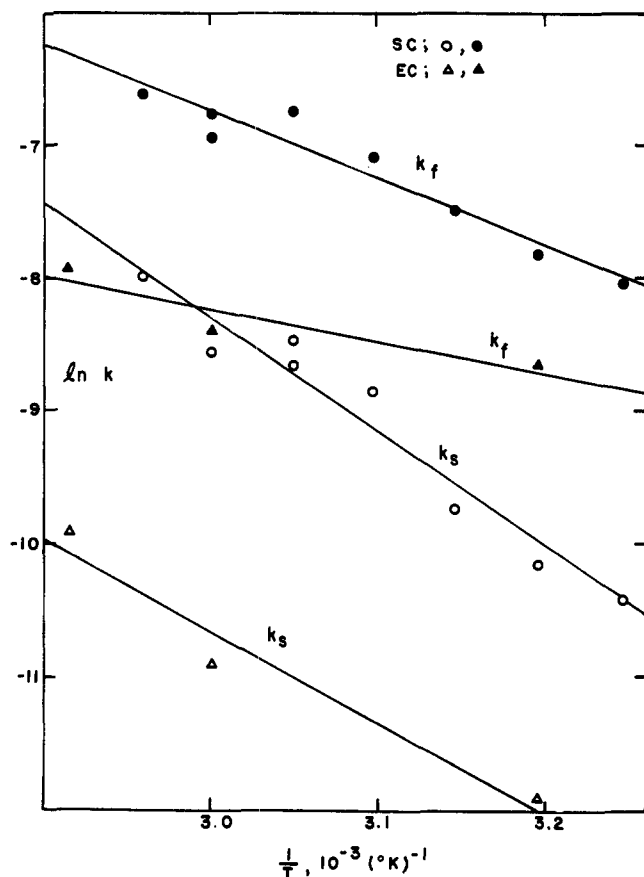


Figure 6. Arrhenius plot of the fast and slow decay constants in the single crystal sample, solid and open circles; and in the extended-chain sample $\alpha_v = 0.036$, sample P-M, solid and open triangles.

mined by the rate of hydrogen atom migration by means of atoms jumping from a saturated $-\text{CH}_2-$ chain to a free radical center, $-\text{CH}_2\dot{\text{C}}\text{HCH}_2-$, as previously postulated¹ and as indicated by the catalytic effect of molecular hydrogen, then the activation energy for the jumping step will be determined by the closeness of approach of the free-radical center to the methylene group in the saturated chain. Dole *et al.*¹² attempted to estimate roughly activation energies for different configurations and different $-\text{CH}$ and $-\text{C}\cdot$ distances, using the potential energy of the CH gaseous diatomic molecule as calculated by a Morse function as a guide. For example, to reduce the activation energy to 10 kcal mol⁻¹ the internuclear distance between the H-atom nucleus on the saturated chain and the vacancy center on the free radical would have to be about 0.4 Å. Possibly the low activation energies in the EC sample may be the result of the formation of these samples under high pressure with a possible compression of the chains in the amorphous zones to closer interchain distances at various locations than in ordinary bulk PE.

An inspection of Figure 6 reveals that the experimental

data for the EC samples are rather scattered and with only three points to compute the slope the E_a values for the EC samples must be considered rather uncertain at the present time.

Also given in Table IV are values of the preexponential factor of the Arrhenius equation. In a normal gas-phase first-order reaction, such as a unimolecular decomposition, the A values have orders of magnitude usually around 10¹³ sec⁻¹; some first-order isomerization reactions, on the other hand, can have A values¹³ as low as 10⁵. Some of the A values of Table IV go as low as 0.3. It is also rather surprising that the A values for the fast component of the alkyl radical decay are lower with one exception than those for the slow decay. If these data are correct, it means that there is a larger negative entropy for the fast decay than for the slow decay in some instances. The physical interpretation of this conclusion is that in the fast decay process in the SC and EC samples the free radicals must make more jumps and wander longer distances before meeting another free radical than do the slowly decaying free radicals. Probably the slow alkyl radical decay is largely by reaction of the free radical with an unsaturated group to form an allyl free radical (see Waterman and Dole⁴). The low activation energy of the fast decay process makes possible the larger number of jumps.

Kusumoto *et al.*¹⁰ also studied alkyl radical decay in γ -irradiated single crystals of polyethylene. They observed a fast and a slow decay, but concluded that their slow decay followed second-order kinetics. However, their slow decay rate was so small that the data would probably have agreed with first-order kinetics equally well. These authors concluded that the slow decay involved "reaction of isolated radicals within the crystal." If this were true, then molecular hydrogen would not have the marked catalytic effect on the slow decay process that is demonstrated by the data of Figure 4. Their slow decay constants decreased with increasing lamellar thickness. If the latter crystals contained a smaller fraction of amorphous polyethylene, this result is in agreement with ours. Densities of their samples were not given. As for the fast decay, Kusumoto *et al.*¹⁰ give an empirical expression to describe their results, but their rapid decay data were independent of lamellar thickness.

Acknowledgments. The research was supported by the U. S. Atomic Energy Commission and by income from the chair in chemistry at Baylor University endowed by a gift from the Robert A. Welch Foundation. The Phillips Petroleum Co. kindly supplied the Marlex-6002 polyethylene and Professor B. Wunderlich of Rensselaer Polytechnic Institute the samples of extended chain PE.

References and Notes

- (1) Paper XII of this series: D. R. Johnson, W. Y. Wen, and M. Dole, *J. Phys. Chem.*, **77**, 2174 (1973).
- (2) T. M. Deas, Jr., H. H. Hofer, and M. Dole, *Macromolecules*, **5**, 223 (1972).
- (3) S. Kubo and M. Dole, submitted for publication.

- (4) D. C. Waterman and M. Dole, *J. Phys. Chem.*, **74**, 1913 (1970).
- (5) A. Keller and D. J. Priest, *J. Macromol. Sci. Phys.*, **2**, 479 (1968).
- (6) P. Ju. Butiagin, *Pure Appl. Chem.*, **30**, 57 (1972).
- (7) M. Dole in "The Radiation Chemistry of Macromolecules," M. Dole, Ed., Academic Press, New York, N. Y. 1972, Vol. I, p 340.
- (8) M. Dole, *Advan. Radiat. Chem.*, **4**, in press.
- (9) C. P. Poole, Jr., "Electron Spin Resonance, A Comprehensive Treatise on Experimental Techniques," Interscience Publishers, New York, N. Y., 1967, p 557.
- (10) N. Kusumoto, T. Yamamoto, and M. Takayanagi, *J. Polym. Sci., Part A-2*, **9**, 1173 (1971).
- (11) W. J. Moore, "Physical Chemistry," Prentice-Hall, Inc., Englewood Cliffs, N. J. 4th ed., 1972, p 163.
- (12) M. Dole, G. G. A. Böhm, and D. C. Waterman, *Eur. Polym. J. Suppl.*, **93** (1969).
- (13) See, for example, A. A. Frost and R. G. Pearson, "Kinetics and Mechanism," John Wiley & Sons, Inc., New York, N. Y., 2nd ed., 1961, p 111.

Electron Spin Resonance Evidence for Dissociative Electron Capture in γ -Irradiated Poly(vinyl chloride)-2-Methyltetrahydrofuran Glassy Solution

Y. J. Chung, S. Yamakawa, and V. Stannett*

Department of Chemical Engineering, North Carolina State University, Raleigh, North Carolina 27607. Received October 15, 1973

ABSTRACT: In the radiolysis of poly(vinyl chloride) (PVC), the predominant process for formation of the primary PVC radical ($-\text{CH}_2\dot{\text{C}}\text{H}-$) has been widely assumed in the literature to be the homolysis of a C-Cl bond. We have found that PVC acts as an electron scavenger to produce the primary PVC radical in γ -irradiated PVC-MTHF glassy solution. Accordingly, it is proposed that dissociative electron capture plays an important role for the formation of the primary PVC radical in the present system. The primary PVC radical is characterized by an esr spectrum of eight equally spaced lines with an average separation of 21.7 G. The analysis of an esr spectrum obtained from the γ -irradiated PVC-MTHF glass has been facilitated by analyzing esr spectra obtained from γ -irradiated bulk 3-chloropentane and 3-chloropentane-MTHF glass.

In the radiolysis of poly(vinyl chloride) (PVC), the primary PVC radical ($-\text{CH}_2\dot{\text{C}}\text{H}-$) has been assumed¹ to be formed through the homolysis of a C-Cl bond. Dissociative electron capture which is a feasible alternative mechanism and has been established² as an important process in the radiolysis of alkyl chlorides, has not been considered in the case of PVC.

To assess the importance of dissociative electron capture in the case of PVC, we have carried out an electron scavenging experiment using PVC as an electron scavenger in 2-methyltetrahydrofuran (MTHF) glass at 77°K. MTHF glass is used in the present study since "trapped electrons" are known³ to form in the γ -irradiated MTHF glass at low temperatures. Furthermore, MTHF is a solvent for PVC and has been found, in our laboratory, to form an excellent glassy solution of PVC at low temperatures. This paper reports esr evidence for dissociative electron capture by PVC during the γ irradiation of MTHF doped with PVC.

Experimental Section

An unplasticized commercial PVC (Sumilit SX-11, $\text{DP}_n = 1100$) supplied by the Sumitomo Chemical Co. was dissolved in tetrahydrofuran (Fisher Certified). After precipitating PVC from a tetrahydrofuran solution with methanol, PVC was washed in methanol, and dried *in vacuo* at room temperature. Eastman White Label MTHF (stabilized with hydroquinone) was distilled under vacuum from sodium and stored over sodium *in vacuo*. In the preparation of PVC-MTHF solution, a measured amount of MTHF was transferred into esr tubes (3-mm i.d.), containing PVC, on a vacuum line. After sealing off *in vacuo*, the tubes were warmed at 318°K for 1 day to dissolve the PVC and then cooled down quickly to 77°K to form a rigid (glassy) solution. 3-Chloropentane was obtained from K & K Laboratories, Inc., and used without further purification. All samples used in the present esr studies were degassed to 10^{-5} mm and sealed off under vacuum. Esr tubes were made from Suprasil tubing supplied by Amersil, Inc., Hillside, N. J. γ Irradiation was carried out in a Gammacell 220 cobalt-60 source (Atomic Energy of Canada Ltd.); the dose rate of the source was 0.6 Mrad/hr. Total irradiation doses given to samples ranged from 0.3 to 1.5 Mrad in order to obtain suitably intense esr spectra. Esr spectra were recorded with an X-

band spectrometer with 100-kHz field modulation (Japan Electron Optics Laboratory Co., Model JES-ME-1X).

Results and Discussion

A γ -irradiated MTHF glass at 77°K is colored blue.³ The blue color disappears on exposure of the sample to visible light from a projector. The upper esr spectrum of Figure 1 shows an esr spectrum of the γ -irradiated MTHF recorded at 77°K in the dark. This esr spectrum consists of a very sharp singlet ($g = 2.003$) and a septet with an average hyperfine splitting (hfs) of 20 G. After recording the esr spectrum shown in the upper part of Figure 1, illumination of the sample *in situ* with visible light caused disappearance of the singlet as shown in the lower esr spectrum of Figure 1. The photobleachable singlet esr spectrum with line width between derivative maxima of 5 G becomes power saturated as the microwave power is raised. These results including the photobleaching, the esr line width and the power saturation of the singlet esr spectrum are characteristic of trapped electrons previously observed⁴ in the γ -irradiated MTHF glass. Accordingly, the singlet esr spectrum is assigned to the trapped electron. The septet esr spectrum is analyzed into a quartet (hfs of 20 G) of doublets (hfs of 20 G) of doublets (hfs of 40 G). The determined hyperfine splittings are in good agreement with the reported⁴ values of MTHF radical.

After γ irradiation at 77°K in the dark, the MTHF glass incorporating 3.5 mol % of PVC is colorless. Before exposing the γ -irradiated sample to visible light, an esr spectrum shown in Figure 2 was recorded at 77°K in the dark. It is analyzed into the nine equally spaced lines with an average separation of 19 G. On illuminating the γ -irradiated sample *in situ* with visible light for 30 min, the nine-line esr spectrum did not show any change, indicating that the singlet esr spectrum attributable to the trapped electron was not present in the nine-line esr spectrum. Thus, it is reasonable to assume PVC acts as an electron scavenger in the γ -irradiated MTHF glass. The nine-line esr spectrum can be analyzed into a doublet (hfs